

Supporting Information

Metal-organic framework (ZIF-67) as efficient cocatalyst for photocatalytic reduction of CO₂: the role of morphology effect

Mang Wang,^a Jinxuan Liu,^{a,*} Chunmei Guo,^a Xiaosu Gao,^a Chenghuan Gong,^a Yan Wang,^b Bo Liu,^b Xiaoxin Li,^a Gagik G. Gurzadyan,^a Licheng Sun^{a, c, *}

^a State Key Laboratory of Fine Chemicals, Institute of Artificial Photosynthesis, Dalian University of Technology, 116024 Dalian, China.

^b Department of Chemistry, KTH Royal Institute of Technology, 110044 Stockholm, Sweden.

*Corresponding author:

E-mail: jinxuan.liu@dlut.edu.cn; sunlc@dlut.edu.cn

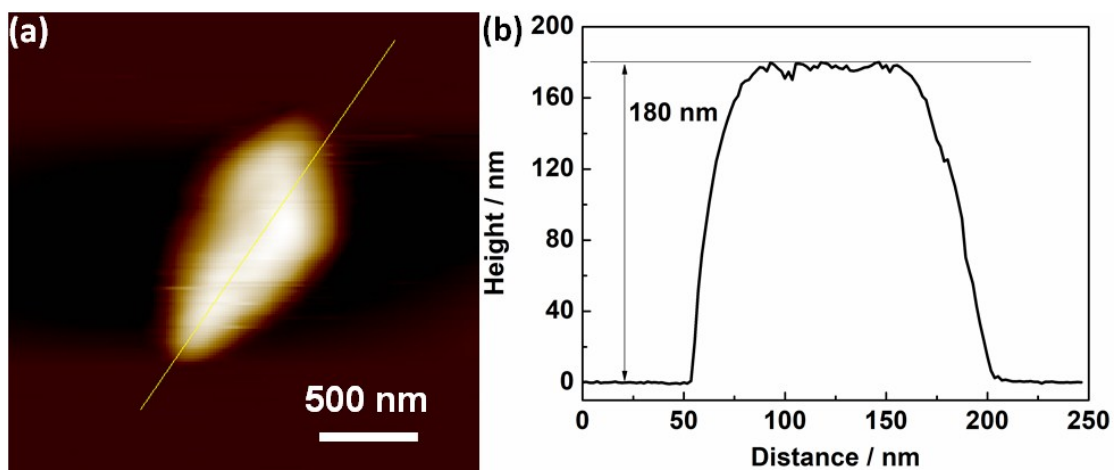


Figure S1. (a) AFM image of ZIF-67_3 and (b) height profile.

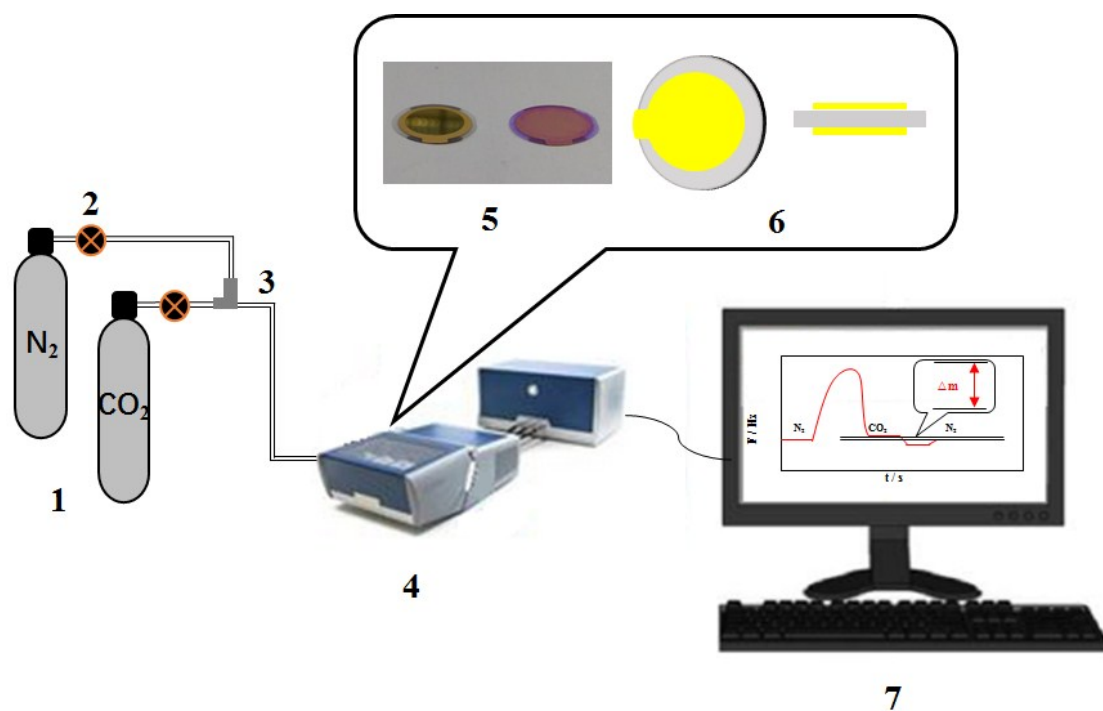


Figure S2. Schematic drawing of in-situ quartz-crystal microbalance setups coupled with high-temperature chamber for CO_2 adsorption. (1) gas supply (N_2 and CO_2); (2) gas flow controller; (3) three-way valve gas distributor; (4) QCM with high temperature chamber; (5) QCM sensor with and without ZIF-67 coating; (6) QCM sensor: top view(left), and cross section(right); (7) computer.

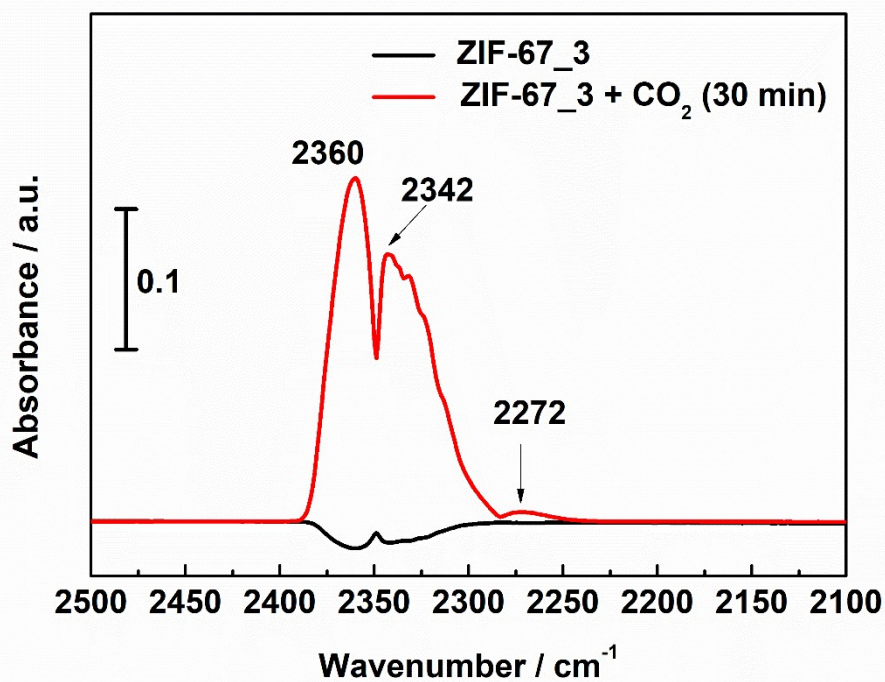


Figure S3. In-situ FTIR spectra recorded with ZIF-67_3 sample with and without CO₂. The solution was continuously bubbled with CO₂ during the measurement. Therefore, the band at 2360 cm⁻¹ and 2342 cm⁻¹ can be attributed to the R branch and P branch of the antisymmetric of CO₂ stretching vibrations, respectively. As can be seen from Figure S3, with the introduction of CO₂, a band at 2272 cm⁻¹ was observed, which can be assigned to asymmetric stretching vibrations of CO₂ molecule adsorbed on Co²⁺.

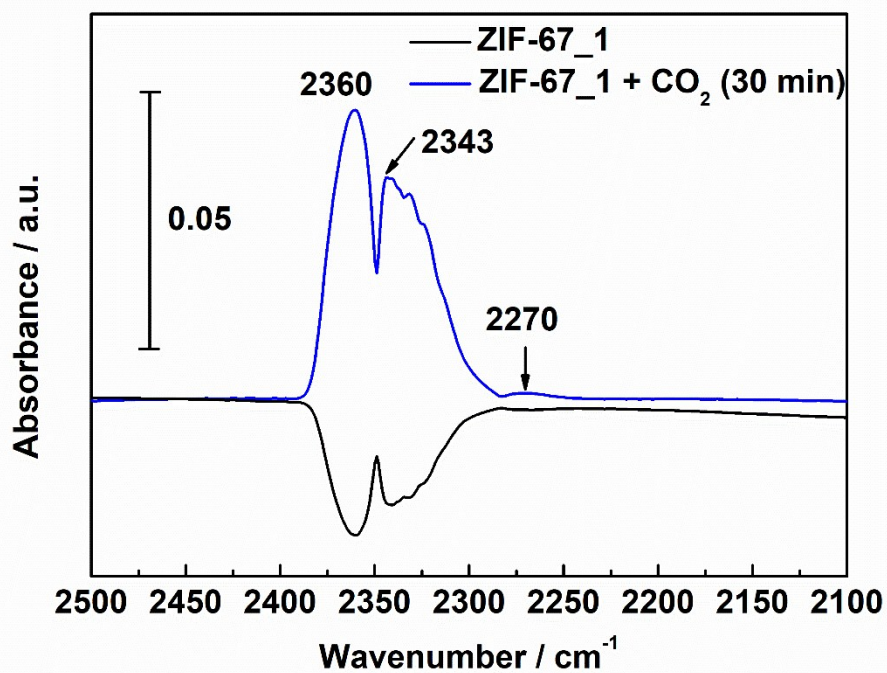


Figure S4. In-situ FTIR spectra recorded with ZIF-67_1 sample with and without CO₂. The solution was continuously bubbled with CO₂ during the measurement. Therefore, the band at 2360 cm⁻¹ and 2343 cm⁻¹ can be attributed to the R branch and P branch of the antisymmetric of CO₂ stretching vibrations, respectively. As can be seen from Figure S4, with the introduction of CO₂, a band at 2270 cm⁻¹ was observed, which can be assigned to asymmetric stretching vibrations of CO₂ molecule adsorbed on Co²⁺.

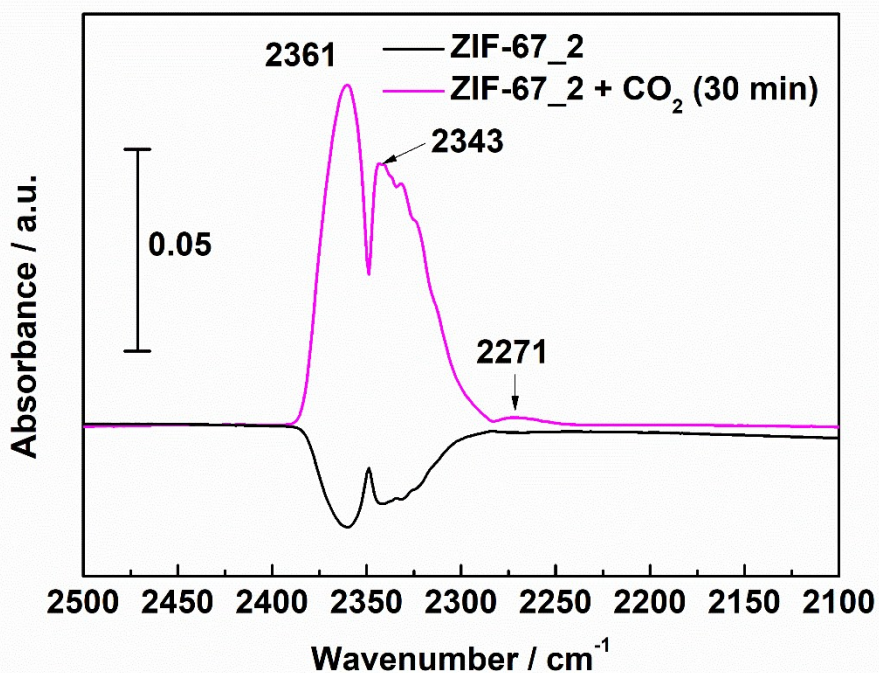


Figure S5. In-situ FTIR spectra recorded with ZIF-67_2 sample with and without CO₂. The solution was continuously bubbled with CO₂ during the measurement. Therefore, the band at 2361 cm⁻¹ and 2343 cm⁻¹ can be attributed to the R branch and P branch of the antisymmetric of CO₂ stretching vibrations, respectively. As can be seen from Figure S5, with the introduction of CO₂, a band at 2271 cm⁻¹ was observed, which can be assigned to asymmetric stretching vibrations of CO₂ molecule adsorbed on Co²⁺.

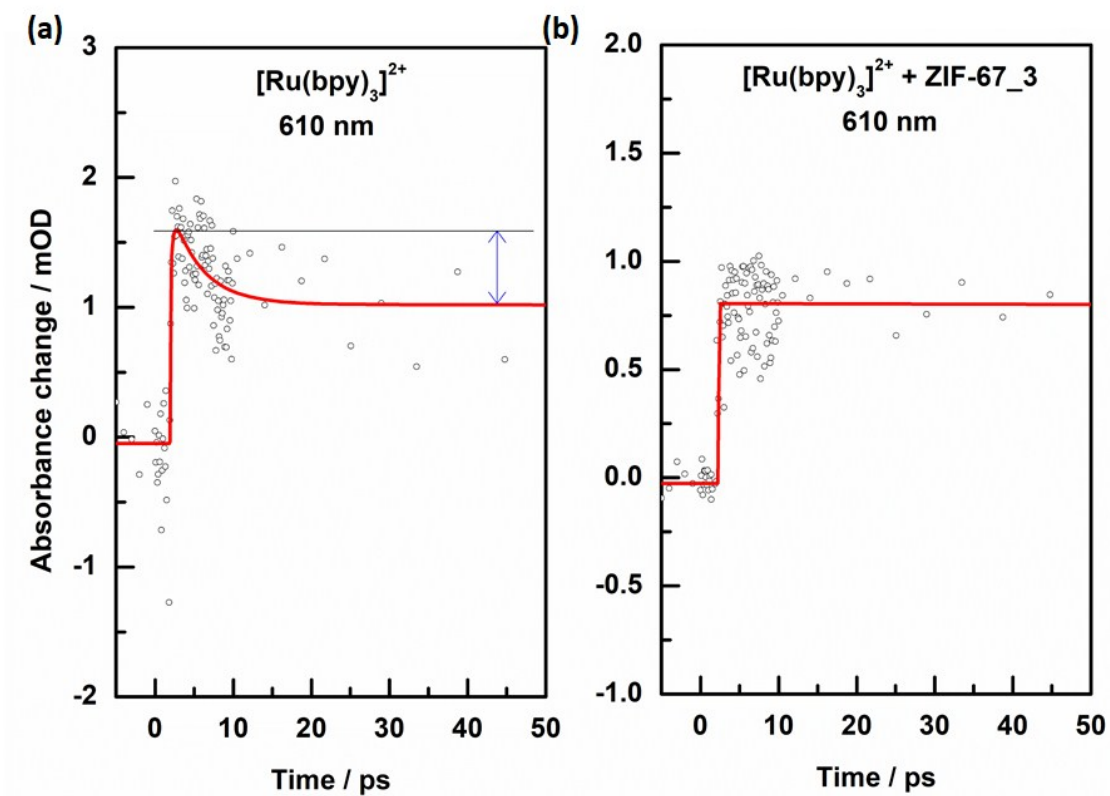


Figure S6. Transient kinetics monitored at 610 nm for $[\text{Ru}(\text{bpy})_3]^{2+}$ and $[\text{Ru}(\text{bpy})_3]^{2+} + \text{ZIF-67}_3$.

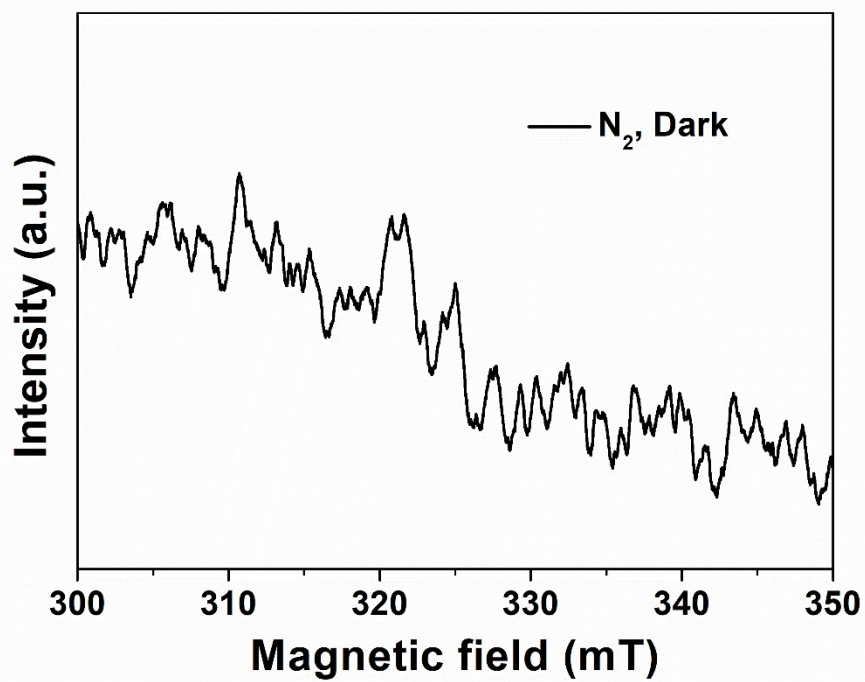


Figure S7. ESR signal of $[\text{Ru}(\text{bpy})_3]^{2+} + \text{ZIF-67}_3$ recorded at 150 K in N_2 without light.

Table S1. Vibrational frequencies of MIM, and the as-synthesized ZIF-67 materials together with their corresponding band assignments.

| Nr. | Band position / cm^{-1} | | Assignment |
|-----|----------------------------------|------------|----------------------------------|
| | MIM | ZIF-67_1-3 | |
| 1 | 680, 741, 754 | 687,754 | $\gamma_{\text{imidazole ring}}$ |
| 2 | 900-1350 | 900-1350 | $\beta_{\text{imidazole ring}}$ |
| 3 | 1372 | 1382 | $\nu_{\text{sym}}\text{CH}_3$ |
| 4 | 1457 | 1481 | $\nu_{\text{assym}}\text{CH}_3$ |
| 5 | 1350-1500 | 1350-1500 | $\nu_{\text{imidazole ring}}$ |
| 6 | 1594 | 1562 | |
| 7 | 1844 | / | $\nu_{\text{N-H}}$ |

Table S2. BET surface area and microporous volume of ZIF-67 of different morphology.

| Sample | $S_{\text{BET}} / \text{m}^2\text{g}^{-1}$ | $V_{\text{pore}} / \text{cm}^3\text{g}^{-1}$ | $V_{\text{micro}} / \text{cm}^3\text{g}^{-1}$ |
|----------|--|--|---|
| ZIF-67_1 | 1698.877 | 0.6924 | 0.581 |
| ZIF-67_2 | 835.704 | 0.3863 | 0.288 |
| ZIF-67_3 | 16.245 | 0.05079 | 0 |

Table S3. Reported MOF materials for converting CO₂ to CO under visible light irradiation.

| MOFs | Condition | | | | Product CO[μ mol] | TON | Ref. |
|--|-----------------|-----------------------|------------------------------|----------|------------------------|------|-----------|
| | Quantity | Light [nm] | Solvent (Sacrificial agent) | Time [h] | | | |
| Co-ZIF-9 | 0.8 μ mol | $\lambda > 420$ | MeCN/H ₂ O (TEOA) | 0.5 | 41.8 | 52.2 | 1 |
| ZIF-67 | 0.45 μ mol | $\lambda > 420$ | MeCN/H ₂ O (TEOA) | 0.5 | 37.4 | 112 | 2 |
| Co-ZIF-9 | 4 μ mol | $\lambda > 420$ | MeCN/H ₂ O (TEOA) | 1 | 50.4 | 12.6 | 3 |
| MOF-1 | | 410 | MeCN/H ₂ O (TEA) | 6 | / | 6.44 | 3b |
| UiO-66/ carbon nitride | 0.1 g | $400 < \lambda < 800$ | MeCN/H ₂ O (TEA) | 6 | 59.4 | / | 4 |
| MOF 4 | 1-2 μ mol | $\lambda > 300$ | MeCN (TEA) | 6 | / | 5 | 5 |
| ZIF-67_3 (ZIF-L) | 4.4 μ mol | $\lambda > 400$ | MeCN/H ₂ O (TEOA) | 3.8 | 15.57 | 3.5 | This work |
| MOF-525-Co | 2 mg | $400 < \lambda < 800$ | MeCN (TEOA) | 6 | 2.25 | / | 6 |
| CPO-27- Mg/TiO ₂ | 10 mg | 365 | water vapor | 10 | 409 | | 7 |
| Ag ₃ Re ₃ - MOF | 0.5-8 μ mol | $400 < \lambda < 700$ | MeCN (TEA) | 50 | / | 2.8 | 8 |
| Re-MOF- (NH ₂)(X%) | 5 mg | $400 < \lambda < 700$ | TEA | 6 | 33 | / | 9 |

References

1. Wang, S.; Yao, W.; Lin, J.; Ding, Z.; Wang, X., Cobalt imidazolate metal-organic frameworks photosplit CO₂ under mild reaction conditions. *Angew Chem Int Ed Engl* **2014**, *53* (4), 1034-8.
2. Qin, J.; Wang, S.; Wang, X., Visible-light reduction CO₂ with dodecahedral zeolitic imidazolate framework ZIF-67 as an efficient co-catalyst. *Applied Catalysis B: Environmental* **2017**, *209*, 476-482.
3. (a) Wang, S.; Wang, X., Photocatalytic CO₂ reduction by CdS promoted with a zeolitic imidazolate framework. *Applied Catalysis B: Environmental* **2015**, *162*, 494-500; (b) Huang, R.; Peng, Y.; Wang, C.; Shi, Z.; Lin, W., A Rhenium-Functionalized Metal-Organic Framework as a Single-Site Catalyst for Photochemical Reduction of Carbon Dioxide. *Eur. J. Inorg. Chem.* **2016**, *2016* (27), 4358-4362.
4. Shi, L.; Wang, T.; Zhang, H.; Chang, K.; Ye, J., Electrostatic Self-Assembly of Nanosized Carbon Nitride Nanosheet onto a Zirconium Metal-Organic Framework for Enhanced Photocatalytic CO₂ Reduction. *Advanced Functional Materials* **2015**, *25* (33), 5360-5367.
5. Wang, C.; Xie, Z.; deKrafft, K. E.; Lin, W., Doping metal-organic frameworks for water oxidation, carbon dioxide reduction, and organic photocatalysis. *J Am Chem Soc* **2011**, *133* (34), 13445-54.
6. Zhang, H.; Wei, J.; Dong, J.; Liu, G.; Shi, L.; An, P.; Zhao, G.; Kong, J.; Wang, X.; Meng, X.; Zhang, J.; Ye, J., Efficient Visible-Light-Driven Carbon Dioxide Reduction by a Single-Atom Implanted Metal-Organic Framework. *Angew. Chem. Int. Ed. Engl.* **2016**, *55* (46), 14310-14314.
7. Wang, M.; Wang, D.; Li, Z., Self-assembly of CPO-27-Mg/TiO₂ nanocomposite with enhanced performance for photocatalytic CO₂ reduction. *Applied Catalysis B: Environmental* **2016**, *183*, 47-52.
8. Choi, K. M.; Kim, D.; Rungtaweeworant, B.; Trickett, C. A.; Barmanbek, J. T.; Alshammari, A. S.; Yang, P.; Yaghi, O. M., Plasmon-Enhanced Photocatalytic CO₂ Conversion within Metal-Organic Frameworks under Visible Light. *J. Am. Chem. Soc.* **2017**, *139* (1), 356-362.
9. Ryu, U. J.; Kim, S. J.; Lim, H. K.; Kim, H.; Choi, K. M.; Kang, J. K., Synergistic interaction of Re complex and amine functionalized multiple ligands in metal-organic frameworks for conversion of carbon dioxide. *Sci Rep* **2017**, *7* (1), 612.